HHS Public Access

Author manuscript

Radiat Res. Author manuscript; available in PMC 2022 June 01.

Published in final edited form as:

Radiat Res. 2021 June 01; 195(6): 590–595. doi:10.1667/RADE-20-00020.1.

In Vitro Radiosensitivity of Murine Marrow Stromal Cells Varies Across Donor Strains

Ashley R. Sweeney-Ambros, **Alexander N. Nappi**, **Megan E. Oest**[1]

Department of Orthopedic Surgery, SUNY Upstate Medical University, Syracuse, New York

Abstract

Mouse models are widely used in the study of musculoskeletal radiobiology both *in vivo* and *in vitro*. Two of the most commonly used mouse strains are C57BL/6 and BALB/c. However, little is known about their equivalence in response to ionizing radiation. In this study we compare the responses of marrow stromal cells derived from both of these strains to X rays *in vitro* at passages 0 and 2. Colony-forming efficiency was significantly higher in BALB/c marrow stromal cells at passage 0. Radiation-induced decreases in colony-forming unit (CFU) formation at passage 0 were comparable across both strains at 0–2 Gy, but BALB/c stromal cells were more radiosensitive than C57BL/6 stromal cells at 3–7 Gy. Osteogenic differentiation at passage 2 was not affected by radiation for either strain. This work demonstrates that commonly used inbred mouse strains differ in their early-passage marrow stromal cell responses to X rays, including self-renewal and differentiation potential. This variability is an important point to consider when selecting an animal model for *in vivo* or *in vitro* study.

INTRODUCTION

Mouse models are widely used to study the effects of radiation therapy on tissues and organs both *in vivo* and *in vitro*. Postirradiation changes in murine bone include loss of strength (1), embrittlement (2), decreased remodeling (3) and depletion of hematopoietic stem cells (HSCs) (4, 5). However, the radiosensitivity of bone marrow stromal cells (MSCs) is not well characterized, despite the important role of these cells in osteogenesis HSC engraftment.

The literature describes radiation effects on MSCs purified by cell sorting or selective passaging *in vitro*, but not MSCs at early passages. MSCs are relatively radioresistant (6) and remain viable even when rendered non-proliferative by radiation treatment (7). Milligray irradiation can induce proliferation of rodent MSCs (8), and loss of viability after 2–10 Gy irradiation *in vitro* (9). *In vivo*, MSCs play a critical role in regulating engraftment and survival of HSCs (10). Bone marrow stromal cells may be depleted or mobilized postirradiation and can later repopulate marrow. Using focal irradiation of the distal femur in mice (5 × 4 Gy), Cao *et al*. (11) demonstrated MSC ablation throughout the femur at one week, with partial recovery of MSCs in the adjacent marrow by four weeks.

[1]Address for correspondence: Department of Orthopedic Surgery, SUNY Upstate Medical University, 3217 Institute for Human Performance, 750 East Adams St., Syracuse, NY 13210; oestm@upstate.edu.

Mouse models of radiation effects on skeletal tissues have mostly used BALB/c (1–3, 12, 13) and C57BL/6 strains (14, 15). While strain-dependent variations in bone micro-architecture, density (16, 17) and MSC function (18) are known, skeletal radiobiology models have not addressed strain variability. Our laboratories have used BALB/cJ mice to study postirradiation changes in bone morphology, composition and biomechanics (1–3, 12, 13). However, the C57BL/6J strain is attractive due to the large number of transgenic modifications available on this background.

The goal of this study was to characterize MSC responses to *in vitro* radiation exposure across three mouse strains, to better inform translation of mechanistic information identified *in vitro* to functional outcomes identified *in vivo*. As a secondary objective, we compared the response of whole marrow cultures at passage 0 (P0) to more purified MSC cultures at passage 2 (P2).

MATERIALS AND METHODS

Animal Model

All methods were approved in advance by the SUNY Upstate Institutional Animal Care and Use Committee. Twelve female mice from each of three strains were used (total n = 36): BALB/cJ (BALB), C57BL6/J (C57) and CB6F1/J (F1) (Jackson Laboratory, Bar Harbor, ME). Mice were euthanized by CO_2 asphyxiation at 12 weeks of age. Disarticulated hindlimbs were stripped of soft tissue and transferred into Hank's buffered salt solution (HBSS) on ice. Marrow for the dose-response study was obtained as dross from another experiment (BALB and C57 mice, 10–16 weeks old, n = 2–4 mice/strain/group, five experimental replicates).

Marrow Stromal Cell Culture

Femurs and tibias were cracked with a sterile mortar and pestle, transferred to a conical tube with HBSS, and pulse vortexed (3 × 3 s) to recover the bone marrow. The cell suspension was passed over a 70-mm nylon mesh. Mononuclear cells were manually counted using a Neubauer chamber with methylene blue dye in 3% acetic acid. The cell suspension was centrifuged (5 min at 300*g*) and resuspended in growth media [MEM-a, 20% fetal bovine serum (FBS), 1% antibiotic/antimycotic (ab/am), 1% GlutaMax™, 100 m*M* 2-mercaptoethanol, 10 n*M* dexamethasone (dex) and 100 m*M* ascorbic acid 2-phosphate (AA2P)].

For expansion, P0 cells were seeded at 0.15–0.25 × 10^6 cells/cm^2 in tissue culture-treated flasks in growth media and placed at 37°C, 5% CO_2. Media was changed every 3–4 days until ~70% confluent. MSCs were selectively passaged with 0.25% Trypsin with 1 m*M* EDTA applied for 3 min at 37°C. Detached cells were collected, pelleted and counted. Passaging from P1 to P2, cells were seeded at 4.5–7.5 × 10^3 cells/cm^2 in flasks.

Colony Forming Unit Assays

For CFU assays, marrow from each animal donor (n = 9/strain) was plated at 50.5 × 10^3 cells/cm^2 (P0) or 50.5 cells/cm^2 (P2) in six-well plates with 5 ml/well growth media. After

24 h, well plates were X-ray irradiated at either 0 or 2 Gy (1.05 Gy/min, 225 kV, 17 mA, turntable on, 55-cm source-to-shelf distance, 0.5-mm copper beam filter; MultiRad 225, Faxitron® Bioptics, Tucson, AZ). MSCs were incubated 12–14 days to permit colony formation. Radiation dose response of primary MSCs was determined by plating P0 cells at 75.0×10^3 cells/cm^2 in T-25 flasks. After 24 h, cells were irradiated at 0, 0.5, 1, 1.5, 2, 3, 4, 5, 6, 7 or 8 Gy as described above, then incubated 12–14 days to permit colony formation.

Colonies were visualized by staining plates with 0.2% crystal violet in methanol. Colonies ≥50 cells were counted manually using a dissecting microscope to aid in morphologically discriminating between MSC colonies and monocyte populations. Colony forming efficiency (CFE) was defined as (number of colonies/number of cells plated). Surviving fraction at 2 Gy (SF2Gy) was defined as (CFE at 2 Gy)/(CFE at 0 Gy).

Osteogenic Differentiation

P2 MSCs were plated at a density of 10.0×10^3 cells/cm^2 into six-well plates containing growth media and cultured to confluence (one week). Growth media was then exchanged for osteogenic media (MEM-α, 10% FBS, 1% ab/am, 1% GlutaMax, 100 m*M* 2-mercaptoethanol, 10 n*M* dex, 100 m*M* AA2P and 5 m*M* b-glycerophosphate), and the cells were irradiated at 2 Gy. Cells were maintained in osteogenic media for 21 days before staining with 40 m*M* alizarin red S (pH 4.1), with calcium deposition quantified using the methods of Gregory *et al.* (19).

Cytokine Arrays

Cells at P0 and P2 from each donor mouse (n = 3 mice/strain) were plated at 31.6×10^3 cells/cm^2 in six-well plates containing 3 ml/well growth media and incubated for 24 h. Media was exchanged for growth media containing only 5% FBS immediately prior to irradiating the well plates at 0 or 2 Gy. Conditioned media was collected at 24 h postirradiation, supplemented with protease inhibitor (10 mg/ml each aprotinin, leupeptin and pepstatin), centrifuged to remove any cellular debris and frozen at −80°C.

Cytokine expression was evaluated using a membrane array (Proteome Profiler Mouse Cytokine Array Panel A, R&D Systems™, Minneapolis, MN) modified for imaging with a LI-COR® Odyssey system (Lincoln, NE) using the manufacturer's protocol for infrared-conjugated dyes. Conditioned media from three mice/strain (total n = 9 mice/strain for three separate experimental replicates) was pooled and processed according to manufacturer protocol. Semi-quantitative analysis of the membrane images was done using ImageJ (National Institutes of Health, Bethesda, MD). For each antibody spot, median density was determined and corrected by subtracting the surrounding median background value. Duplicate spot values were averaged. Relative change in cytokine level was calculated as [(treated sample − stale media)/(stale media)] (Fig. 1). Reactome (reactome.org version 68) (20, 21) was used to conduct overrepresentation analyses for these cytokines.

Statistics

All statistical analyses were performed using JMP13 software. Data were analyzed using analysis of variance (ANOVA) and Tukey's honestly significant difference (THSD) tests.

Data normality was assessed using the Shapiro-Wilk test. All CFE data were normally distributed. Osteogenesis data for C57 MSCs irradiated at 2 Gy was non-normal ($P = 0.0453$).

RESULTS

Colony-Forming Efficiency

Colony-forming efficiency at P0 varied by strain ($P = 0.0098$ by ANOVA). C57 MSCs had a lower CFE than BALB cells (Fig. 2A, $P = 0.0077$ by THSD for P0, 0 Gy group). Radiation significantly decreased CFE only in C57 MSCs ($P = 0.0320$ for 0 Gy vs. 2 Gy by THSD). At P2, strain was not a significant variable as determined by ANOVA (Fig. 2B). Radiation treatment decreased CFE at P2 only in BALB MSCs ($P = 0.0430$ for 0 Gy vs. 2 Gy by THSD).

The effect of increasing radiation dose (0–8 Gy) on CFE was determined for BALB and C57 MSCs at P0. BALB MSCs had an overall higher CFE than C57 cells (Fig. 3A). ANOVA using a regression model demonstrated strain, radiation dose, and their interaction term were significant ($P < 0.0001$ for all). Dose-dependent decreases in CFE were equivalent between the strains for low-dose (0–2 Gy) radiation ($P = 0.0782$ by ANOVA). At higher radiation doses (3–7 Gy), however, the CFE of BALB MSCs decreased more rapidly than in C57 cells ($P = 0.0011$ by ANOVA). Only C57-derived MSCs demonstrated a difference in SF2Gy between passages, with P2 cultures having significantly higher survivorship than P0 cultures (Fig. 3C, $P = 0.0019$ by THSD). The D_0 value (radiation dose that reduces survival to 37%) was calculated to be 3.3 Gy for the BALB MSCs and 2.9 Gy for the C57 MSCs (Fig. 3C).

Differentiation

Osteogenic differentiation at P2 varied significantly by donor strain in both the control (Fig. 4, 0 Gy, $P = 0.0125$ by ANOVA) and irradiated groups ($P = 0.0362$ by ANOVA). At both 0 and 2 Gy, BALB MSCs deposited significantly less mineral than C57 MSCs ($P = 0.0093$ for 0 Gy and $P = 0.0290$ for 2 Gy, THSD). Radiation nor strain were significant factors in mineral deposition for F1 MSCs (Fig. 4).

Cytokine Arrays

Cytokine expression in MSC conditioned media was evaluated 24 h postirradiation. In P2 versus P0 cultures, BLC, KC, IL-1ra, JE, M-CSF, Timp-1, MIP-1a and MIP-1b were consistently increased across both irradiated and nonirradiated groups (Fig. 1). The only exception was with IL-1ra, which was increased in P2 vs. P0 conditioned media, except in C57 MSCs in the 0 Gy irradiated group. Radiation-induced changes in cytokine content of conditioned media were more variable, with most changes occurring in passaged cells. Both BALB and F1 donors at P2 had a decrease in M-CSF, while only F1 donors had a decrease in BLC and an increase in JE. Irradiated C57 MSCs at P2 had an increase in KC with decreases in TIMP-1, JE and MIP-1a.

Pathway overrepresentation analysis was then conducted for the cytokines listed in Fig. 1 using Reactome, an open-source web-based pathway database. Analyses were run only for

passaging-associated cytokines (BLC, KC, IL-1ra, JE, M-CSF, TIMP-1, MIP-1a, MIP-1b), as radiation-associated cytokines were not consistent. Approximately 87.5% of the pathways fell under the Immune System cluster, including IL-10 signaling, and 62.5% fell under the Signal Transduction cluster, of which all five entities were associated with GPCR signaling. The Extracellular Matrix Organization and Hemostasis clusters each contained 12.5% of the passaging-associated overrepresented pathways, and the Metabolism of Proteins cluster contained 37.5% of pathways.

DISCUSSION

MSCs *in vivo* reside within a heterogeneous milieu of cell types, and play a key role in regulating bone homeostasis and HSC function after irradiation. Data presented here highlight the strain-dependent differences in MSC radiosensitivity at early passages. Relatively little is known about the response of murine MSCs to radiation at early passages *in vitro*.

Sugrue *et al*. found that MSCs from C57 mice demonstrated dose-dependent radiosensitivity at 0–10 Gy, analogous to the results presented here (9). Sensitivity of BALB MSCs to 12 Gy irradiation was demonstrated by Clavin *et al*. (22), where increased dose fractionation was found to better maintain early-passage MSC function. Our data indicate that a response to radiation, particularly in the 3–7 Gy range, may vary by mouse strain, as BALB MSCs were more radiosensitive to 3–7 Gy doses and had a lower D_0 value (by 0.4 Gy) than C57 MSCs. Osteogenesis at P2 was unaffected by 2 Gy irradiation for either strain, although that result may be an artifact of growing MSCs to confluence prior to differentiation. This observation aligns with literature suggesting that irradiated MSCs may remain viable but non-proliferative.

The effect of radiation on MSCs has implications not only for maintenance of marrow progenitor cells, but also systemic inflammation, bone remodeling, and regulation of tumor growth and metastasis. It is well established that MSCs can enhance HSC engraftment (23, 24), and it is thought that intramedullary adiposity tissue may abrogate HSC marrow repopulation postirradiation (4). Previously we have shown that unilateral hindlimb irradiation in mice results in loss of bone strength at the contralateral nonirradiated site, suggesting a systemic skeletal response to radiation (1). Data presented here suggest that MSCs may contribute to systemic bone responses via activation of immune signaling pathways, notably IL-10 signaling.

Although P0 MSCs recapitulate the *in vivo* marrow environment more accurately than P2 MSCs, a major drawback is that the presence of other cells in the marrow creates greater variability. Our data suggest a more pronounced effect of cell passaging on inflammatory cytokine expression than radiation-associated cytokine expression. Passaging-associated cytokine differences seen only at P2 may also have an effect on osteogenesis after irradiation (conducted on P2 MSCs) in which no differences were observed (Fig. 4). Taken together, MSC passage number, along with mouse strain, is a potentially confounding variable that needs to be controlled for in the design of future studies.

The goals of this work were to evaluate MSC responses to radiation *in vitro* across three mouse strains and identify ways in which radiosensitivity varied between MSC monoculture at P2 compared to heterogeneous P0 cultures. Data presented here suggest that BALB and C57 MSCs differ in CFE, radiosensitivity, and osteogenesis at P2. MSCs derived from F1 mice generally represented a median outcome between the other strains. C57 MSCs had significantly increased survivorship at P2 compared to P0, while there were no passage-associated changes in SF2Gy for the BALB or F1 strains. Collectively, these data suggest strain-dependent differences in MSC responses to radiation may factor into *in vivo* outcomes.

ACKNOWLEDGMENTS

Research reported in this publication was supported by the National Institute of Arthritis and Musculoskeletal and Skin Diseases of the National Institutes of Health (NIH) under award no. R01AR070142 (M.E.O.). The content is the sole responsibility of the authors and does not necessarily represent the official views of the NIH.

REFERENCES

1. Oest ME, Policastro CG, Mann KA, Zimmerman ND, Damron TA. Longitudinal effects of single hindlimb radiation therapy on bone strength and morphology at local and contralateral sites. J Bone Miner Res 2018; 33:99–112. [PubMed: 28902435]
2. Bartlow CM, Mann KA, Damron TA, Oest ME. Limited field radiation therapy results in decreased bone fracture toughness in a murine model. PloS One 2018; 13:e0204928. [PubMed: 30281657]
3. Oest ME, Franken V, Kuchera T, Strauss J, Damron TA. Long-term loss of osteoclasts and unopposed cortical mineral apposition following limited field irradiation. J Orthop Res 2015; 33:334–42. [PubMed: 25408493]
4. Green DE, Rubin CT. Consequences of irradiation on bone and marrow phenotypes, and its relation to disruption of hematopoietic precursors. Bone 2014; 63C:87–94.
5. Li X, Cui W, Hull L, Smith JT, Kiang JG, Xiao M. Effects of low-to-moderate doses of gamma radiation on mouse hematopoietic system. Radiat Res 2018; 190:612–22. [PubMed: 30311842]
6. Singh S, Kloss FR, Brunauer R, Schimke M, Jamnig A, Greiderer-Kleinlercher B, et al. Mesenchymal stem cells show radioresistance in vivo. J Cell Mol Med2012; 16:877–87. [PubMed: 21762375]
7. Cmielova J, Havelek R, Soukup T, Jiroutova A, Visek B, Suchanek J, et al. Gamma radiation induces senescence in human adult mesenchymal stem cells from bone marrow and periodontal ligaments. Int J Radiat Biol 2012; 88:393–404. [PubMed: 22348537]
8. Liang X, So YH, Cui J, Ma K, Xu X, Zhao Y, et al. The low-dose ionizing radiation stimulates cell proliferation via activation of the MAPK/ERK pathway in rat cultured mesenchymal stem cells. J Radiat Res 2011; 52:380–6. [PubMed: 21436606]
9. Sugrue T, Lowndes NF, Ceredig R. Hypoxia enhances the radioresistance of mouse mesenchymal stromal cells. Stem Cells 2014; 32:2188–200. [PubMed: 24578291]
10. de Araujo Farias V, O'Valle F, Lerma BA, Ruiz de Almodovar C, Lopez-Penalver JJ, Nieto A, et al. Human mesenchymal stem cells enhance the systemic effects of radiotherapy. Oncotarget 2015; 6:31164–80. [PubMed: 26378036]
11. Cao X, Wu X, Frassica D, Yu B, Pang L, Xian L, et al. Irradiation induces bone injury by damaging bone marrow microenvironment for stem cells. Proc Natl Acad Sci U S A 2011; 108:1609–14. [PubMed: 21220327]
12. Oest ME, Gong B, Esmonde-White K, Mann KA, Zimmerman ND, Damron TA, et al. Parathyroid hormone attenuates radiation-induced increases in collagen crosslink ratio at periosteal surfaces of mouse tibia. Bone 2016; 86:91–7. [PubMed: 26960578]

13. Oest ME, Mann KA, Zimmerman ND, Damron TA. Parathyroid hormone (1–34) transiently protects against radiation-induced bone fragility. Calcif Tissue Int 2016; 98:619–30. [PubMed: 26847434]
14. Willey JS, Lloyd SA, Robbins ME, Bourland JD, Smith-Sielicki H, Bowman LC, et al. Early increase in osteoclast number in mice after whole-body irradiation with 2 Gy X rays. Radiat Res 2008; 170:388–92. [PubMed: 18763868]
15. Wright LE, Buijs JT, Kim HS, Coats LE, Scheidler AM, John SK, et al. Single-limb irradiation induces local and systemic bone loss in a murine model. J Bone Miner Res 2015; 30:1268–79. [PubMed: 25588731]
16. Beamer WG, Donahue LR, Rosen CJ, Baylink DJ. Genetic variability in adult bone density among inbred strains of mice. Bone 1996; 18:397–403. [PubMed: 8739896]
17. Sabsovich I, Clark JD, Liao G, Peltz G, Lindsey DP, Jacobs CR, et al. Bone microstructure and its associated genetic variability in 12 inbred mouse strains: microCT study and in silico genome scan. Bone 2008; 42:439–51. [PubMed: 17967568]
18. Peister A, Mellad JA, Larson BL, Hall BM, Gibson LF, Prockop DJ. Adult stem cells from bone marrow (MSCs) isolated from different strains of inbred mice vary in surface epitopes, rates of proliferation, and differentiation potential. Blood 2004; 103:1662–8. [PubMed: 14592819]
19. Gregory CA, Gunn WG, Peister A, Prockop DJ. An Alizarin red-based assay of mineralization by adherent cells in culture: comparison with cetylpyridinium chloride extraction. Anal Bio-chem 2004; 329:77–84.
20. Fabregat A, Jupe S, Matthews L, Sidiropoulos K, Gillespie M, Garapati P, et al. The reactome pathway knowledgebase. Nucleic Acids Res 2018; 46:D649–55. [PubMed: 29145629]
21. Fabregat A, Sidiropoulos K, Viteri G, Forner O, Marin-Garcia P, Arnau V, et al. Reactome pathway analysis: a high-performance in-memory approach. BMC Bioinformatics 2017; 18:142. [PubMed: 28249561]
22. Clavin NW, Fernandez J, Schonmeyr BH, Soares MA, Mehrara BJ. Fractionated doses of ionizing radiation confer protection to mesenchymal stem cell pluripotency. Plast Reconstr Surg 2008; 122:739–48. [PubMed: 18766036]
23. Fernandez-Garcia M, Yanez RM, Sanchez-Dominguez R, Her-nando-Rodriguez M, Peces-Barba M, Herrera G, et al. Mesenchymal stromal cells enhance the engraftment of hematopoietic stem cells in an autologous mouse transplantation model. Stem Cell Res Ther 2015; 6:165. [PubMed: 26345192]
24. Kim A, Shim S, Kim MJ, Myung JK, Park S. Mesenchymal stem cell-mediated Notch2 activation overcomes radiation-induced injury of the hematopoietic system. Sci Rep 2018; 8:9277. [PubMed: 29915190]

Relative change in cytokine production [(treatment – stale media)/(stale media)]

Strain	C57		BALB		F1		C57		BALB		F1	
Passage	0						2					
Treatment	Sham	RTx	Sham	RTx	Sham	RTx	Sham	RTx	Sham	RTx	Sham	RTx
BLC	-0.07	-0.25	-0.20	-0.51	-0.63	0.26	2.23	2.33	2.31	2.20	16.51	13.17
C5/C5a	0.15	-0.16	0.01	-0.48	-0.57	0.21	0.03	-0.18	-0.03	0.12	0.26	0.05
IL-3	0.18	-0.07	0.02	-0.42	-0.54	0.25	0.02	-0.41	-0.21	-0.26	0.02	-0.19
IL-4	0.54	-0.14	-0.09	-0.40	-0.58	0.22	-0.34	-0.42	-0.26	-0.30	-0.13	-0.27
IP-10	0.11	-0.09	-0.02	-0.35	-0.54	0.48	-0.26	-0.36	0.59	0.32	0.96	0.28
I-TAC	0.59	0.01	0.07	-0.37	-0.58	0.28	-0.45	-0.40	-0.24	-0.27	0.10	-0.21
TARC	0.10	-0.30	-0.01	-0.02	-0.56	0.33	-0.39	-0.44	-0.30	-0.35	0.07	-0.20
TIMP-1	0.15	-0.16	-0.03	-0.35	-0.56	0.43	5.37	1.00	0.99	0.94	1.00	1.04
G-CSF	0.11	-0.10	-0.04	-0.31	-0.46	0.29	-0.23	-0.25	-0.12	-0.22	0.24	-0.05
GM-CSF	0.24	0.12	0.57	0.02	-0.38	0.34	0.06	-0.01	0.17	-0.08	0.29	0.05
IL-5	0.22	-0.06	0.19	-0.17	-0.44	0.59	-0.25	-0.38	-0.21	-0.24	0.22	-0.11
IL-6	0.30	0.05	0.25	0.01	-0.39	0.39	0.01	0.96	0.78	0.86	0.47	0.18
KC	0.04	-0.23	0.06	-0.19	-0.44	0.31	6.28	13.24	10.96	12.39	8.81	8.24
M-CSF	0.64	0.04	0.14	-0.27	-0.48	0.43	14.39	14.54	18.38	16.00	23.93	16.94
TNF-a	0.33	-0.12	-0.02	-0.08	-0.28	0.70	-0.02	-0.14	0.26	0.30	0.41	-0.04
TREM-1	0.27	-0.06	0.13	-0.23	-0.43	0.69	-0.22	-0.33	0.04	-0.12	0.51	-0.01
I-309	0.30	-0.02	0.16	-0.24	-0.45	0.29	1.19	0.20	2.18	1.12	0.27	-0.11
Eotaxin	0.37	0.07	0.24	-0.07	-0.35	0.45	0.13	0.11	0.33	0.29	0.69	0.15
IL-7	0.38	-0.07	0.08	-0.36	-0.57	0.36	-0.30	-0.30	-0.03	-0.11	0.29	-0.11
IL-10	0.43	-0.04	0.10	-0.05	-0.36	0.36	0.13	0.11	0.57	0.30	0.65	0.02
JE	0.31	-0.02	0.19	-0.19	-0.43	0.47	18.94	3.39	3.39	3.27	3.44	21.40
MCP-5	0.76	0.10	0.13	-0.02	-0.15	0.60	-0.12	-0.38	0.01	-0.12	0.22	-0.31
sICAM-1	0.40	-0.01	0.12	-0.22	-0.39	0.25	-0.12	-0.34	-0.06	-0.14	0.29	-0.17
IFNg	0.32	-0.14	0.08	-0.33	-0.52	0.32	-0.23	-0.09	0.01	-0.08	0.39	-0.10
IL-13	0.63	0.05	0.02	-0.27	-0.49	0.26	-0.36	-0.31	-0.08	-0.17	0.09	-0.22
IL-12p70	0.25	-0.01	0.04	-0.18	-0.41	0.23	-0.20	-0.16	0.12	0.81	0.41	-0.08
MIG	0.49	-0.02	0.15	-0.30	-0.51	0.43	-0.21	-0.24	-0.06	-0.12	0.42	-0.06
MIP-1a	0.50	0.03	0.11	-0.30	-0.48	0.33	7.00	4.68	5.75	6.00	2.11	1.40
Il-1a	0.47	-0.02	-0.14	-0.19	-0.06	0.43	0.01	-0.08	0.69	1.10	0.24	-0.02
Il-1b	0.56	0.15	0.03	-0.26	-0.50	0.29	-0.38	-0.29	0.10	0.11	0.19	-0.14
IL-16	0.58	0.16	0.06	-0.17	-0.33	0.53	-0.27	-0.38	0.19	-0.05	0.22	-0.18
IL-17	0.80	0.07	0.06	-0.31	-0.49	0.36	-0.39	-0.28	0.06	-0.07	0.31	-0.08
MIP-1b	0.45	0.08	0.01	-0.19	-0.28	0.29	1.72	0.90	2.26	2.02	0.95	0.57
MIP-2	0.84	0.09	0.05	-0.23	-0.50	0.34	-0.12	0.53	0.46	0.32	0.54	0.12
IL-1ra	0.29	0.15	0.04	-0.35	-0.46	0.16	3.19	3.48	3.44	3.31	3.72	3.77
IL-2	0.27	-0.18	-0.22	-0.48	-0.48	0.01	-0.27	-0.32	0.29	-0.07	0.16	-0.25
IL-23	0.43	0.04	-0.06	-0.39	-0.37	0.22	0.09	0.06	0.38	0.00	0.52	-0.09
IL-27	1.57	0.15	0.07	-0.37	-0.51	0.40	-0.35	-0.31	-0.02	-0.06	0.23	-0.09
RANTES	0.29	-0.06	0.10	-0.35	-0.47	0.37	0.47	0.53	0.45	0.20	0.82	0.47
SDF-1	0.89	0.29	-0.31	-0.49	-0.14	0.26	1.44	0.39	-0.50	-0.51	-0.48	-0.48

decrease *no change* *increase*

FIG. 1.

Cytokine changes in MSC conditioned media associated with radiation and passaging represented as a heat map, with data expressed as relative change from stale media controls.

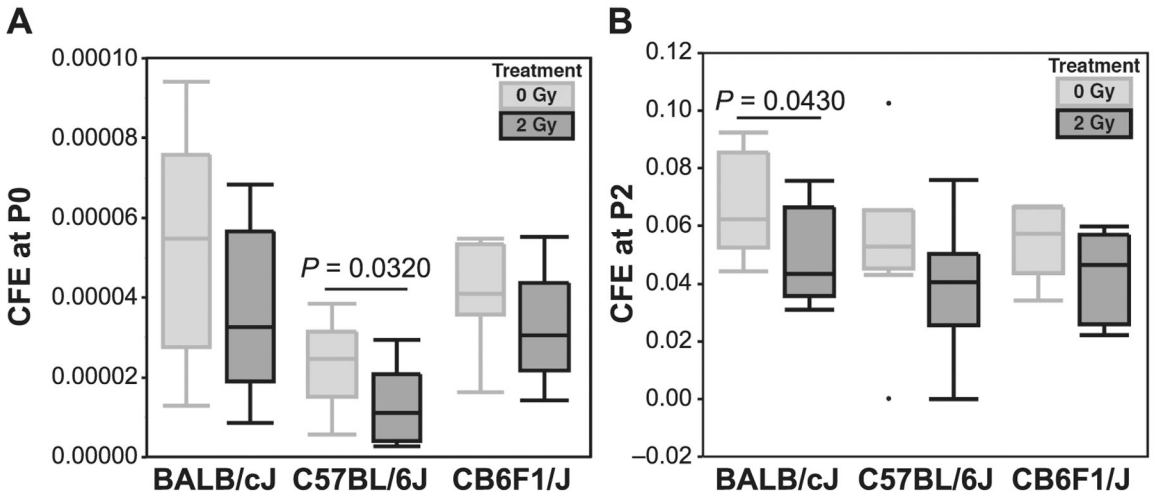

FIG. 2.

Panel A: At P0, radiation decreased mean colony-forming efficiency (CFE) for all strains, although the difference was significant only for C57 MSCs. Panel B: Radiation diminished mean CFE for all strains at P2, although the difference was significant only for BALB MSCs. Data are shown as quartile box plots, central horizontal bar represents median value, outliers are represented as dots.

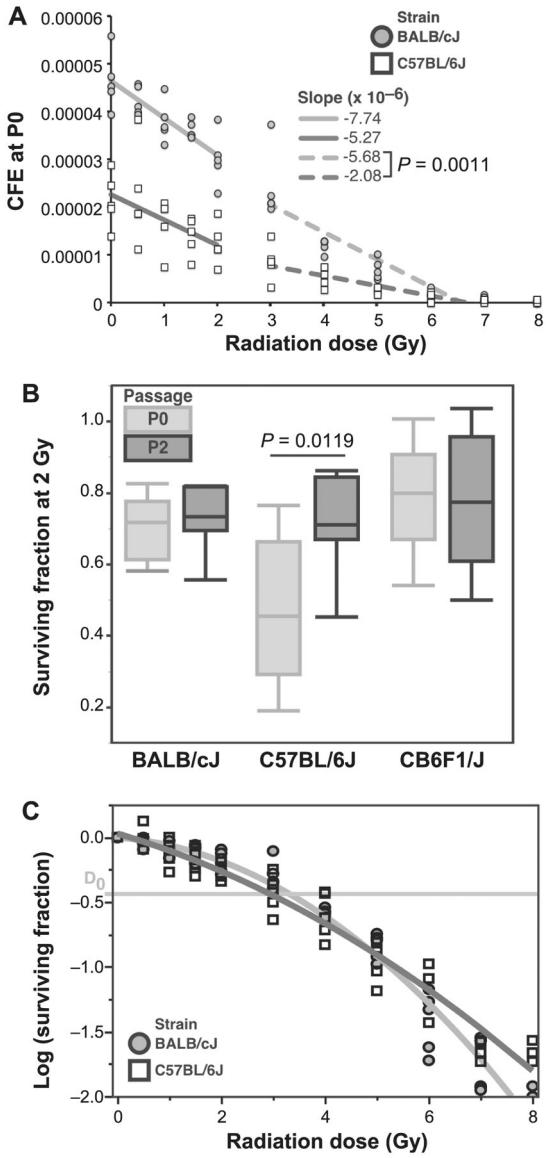

FIG. 3.

Panel A: Colony-forming efficiency (CFE) at P0 as a function of radiation dose. BALB MSCs had a higher initial CFE than C57 cells, but sensitivity to ≤2 Gy radiation was similar between the strains. At higher doses (3–7 Gy), BALB MSCs demonstrated increased radiosensitivity compared to C57 cells. Irradiation at 8 Gy was almost uniformly lethal. Panel B: Surviving fraction at the 2 Gy dose (SF2Gy) for MSCs at P0 and P2. Both BALB and F1 MSCs had similar SF2Gy results for P0 and P2 cultures. However, MSCs from C57 mice had significantly increased SF2Gy at P2 compared to P0. Panel C: SF2Gy as a function of radiation dose represented in a semi-log plot. BALB MSCs had a lower D_0 value (3.3 Gy) than C57 MSCs (2.9 Gy).

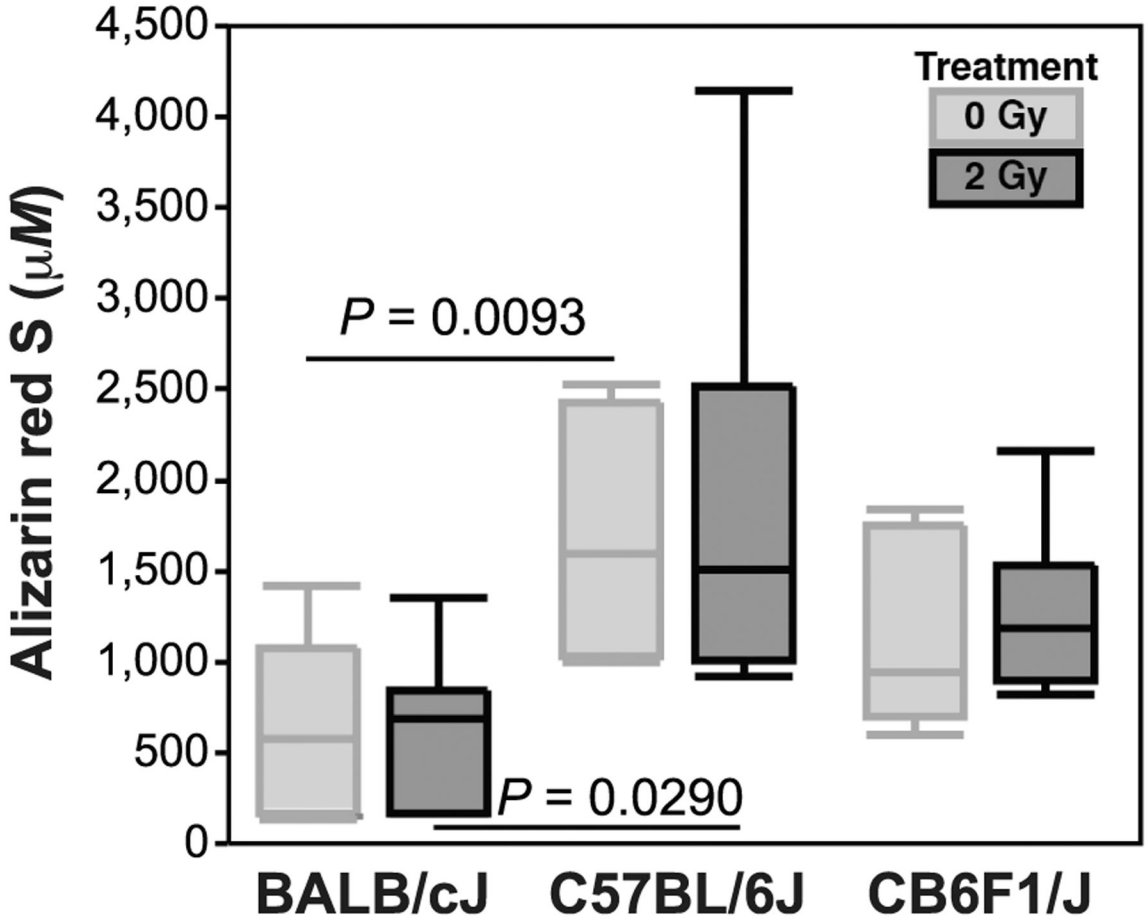

FIG. 4.

Osteogenesis was measured by seeding six-well plates with P2 MSCs at a density of 10.0 × 10^3 cells/cm^2 and differentiating confluent cells in pro-osteogenic media for 21 days (quantified by Alizarin Red S at P2). Mineral deposition differed between BALB and C57 strains, but was unaffected by *in vitro* irradiation, while no significant change was observed in F1 MSCs.